Acta Geologica Sinica (English Edition), 2021, 95(6): 1882–1891

Catalog of Enhanced Geothermal Systems based on Heat Sources

KONG Yanlong[1, 2, 3, *], PAN Sheng[4], REN Yaqian[1, 2, 3], ZHANG Weizun[1, 5], WANG Ke[1, 2, 3], JIANG Guangzheng[6], CHENG Yuanzhi[1, 2, 3], SUN Wenjie[5], ZHANG Chao[6], HU Shengbiao[1, 2, 3] and HE Lijuan[1, 2, 3]

[1] *Key Laboratory of Shale Gas and Geoengineering, Institute of Geology and Geophysics, Chinese Academy of Sciences, Beijing 100029, China*
[2] *Innovation Academy for Earth Science, CAS, Beijing 100029, China*
[3] *College of Earth and Planetary Sciences, University of Chinese Academy of Sciences, Beijing 100049, China*
[4] *Institute of Tibetan Plateau Research of the Chinese Academy of Sciences, Beijing 100085, China*
[5] *College of Geoscience and Surveying Engineering, China University of Mining and Technology, Beijing 100083, China*
[6] *College of Energy, Chengdu University of Technology, Chengdu 610059, China*

Abstract: It is common sense that a deeper well implies higher temperature in the exploration of deep geothermal resources, especially with hot dry rock (HDR) geothermal resources, which are generally exploited in terms of enhanced geothermal systems (EGS). However, temperature is always different even at the same depth in the upper crust due to different heat sources. This paper summarizes the heat sources and classifies them into two types and five sub-types: crust-origin (partial melting, non-magma-generated tectonic events and radiogenic heat production), and mantle-origin (magma and heat conducted from the mantle). A review of global EGS sites is presented related to the five sub-types of heat sources. According to our new catalog, 71% of EGS sites host mantle-origin heat sources. The temperature logging curves indicate that EGS sites which host mantle-origin magma heat sources have the highest temperature. Therefore, high heat flow (>100 mW/m^2) regions with mantle-origin magma heat sources should be highlighted for the future exploration of EGS. The principle to identify the heat source is elucidated by applying geophysical and geochemical methods including noble gas isotope geochemistry and lithospheric thermal structure analysis. This analytical work will be helpful for the future exploration and assessment of HDR geothermal resources.

Key words: geothermal resources, enhanced geothermal systems, heat source, hot dry rock, catalog

Citation: Kong et al., 2021. Catalog of Enhanced Geothermal Systems based on Heat Sources. Acta Geologica Sinica (English Edition), 95(6): 1882–1891. DOI: 10.1111/1755-6724.14876

1 Introduction

Geothermal energy emanates from the interior of the earth. The heat source is mainly composed of residual mantle heat and the radiogenic heat in the crust (Wang, 2015). It has the advantages of great amount, constancy and cleanliness. Its utilization is almost carbon dioxide (CO_2) emission-free, which makes it very popular in the new era to access the target to peak CO_2 emissions and achieve carbon neutrality. Actually, in the past 20 years, global geothermal power generation and direct use have developed very fast, with the installed global capacity reaching 15950.46 MWe and 107727 MWt in 2019 (Huttrer, 2020; Lund and Toth, 2020).

With the increment of total geothermal energy consumption, large-scale geothermal fields are more and more used. Meanwhile, deeper geothermal energy is gradually targeted, with deep hot dry rock (HDR) geothermal resources regarded as the future of geothermal energy. It is estimated that in the USA, the extractable portion of HDR geothermal energy exceeds 200,000 exajoules (EJ) or about 2,000 times the annual consumption of primary energy in the USA in 2005 (Tester et al., 2006), whereas in China, the extractable portion is more than 410,000 EJ or about 4,400 times the consumption of primary energy in China in 2010 (Wang et al., 2012a). Naturally, the question emerges for the exploitation of HDR geothermal energy, where is it and how is the heat accumulated?

Generally, scientists think that it will be hot enough or there will be HDR geothermal energy as long as we drill deeply enough. However, the depth is constrained by the economics, and thus, we have to find economical HDR geothermal reservoirs at shallow depth. At the same depth, we should find a higher temperature region. The success in exploiting high-temperature HDR geothermal energy depends on a comprehensive understanding of the geological structures (Huang and Liu, 2010; Moeck, 2014; Tomac and Sauter, 2018; Jolie et al., 2021). Therefore, all factors from the geological viewpoint should be attached importance, including heat sources, heat flow patterns, fractures and faults, fluid flow patterns and properties of

* Corresponding author. E-mail: ylkong@mail.iggcas.ac.cn

geological formations (Jolie et al., 2021). In the early stage of HDR geothermal energy exploration, heat sources and heat flow pattern should first be identified because they help in targeting the high-temperature zone. In addition, the rock types should be considered, keeping in mind that geothermal reservoirs can be hosted in multiple rock types with different thermal properties. Finally, faults also play a key role in the transportation of fluid and heat (Kong et al., 2020b; Pan et al., 2021), and many high-temperature geothermal systems reside in fault interaction zones (Jolie et al., 2021). Among all the above-mentioned factors, heat sources have a fundamental influence on the distribution of subsurface temperature, whether the geothermal system has high-temperature or not. For example, most of the high-temperature geothermal systems are located in volcanic provinces, since magmatism is an efficient way to transfer heat (Jolie et al., 2021). Therefore, the identification of heat sources is a crucial step in the exploration of HDR geothermal energy. In other words, the regions that have excellent heat sources should be highlighted, and the primary scientific question turns to look for the heat sources.

In the past 40 years of HDR exploration, more than 30 HDR or enhanced geothermal systems (EGS) projects have been done within a depth less than 5 km and temperature between 150°C and 400°C (Breede et al., 2013; Kumari and Ranjith, 2019). Nevertheless, at least to our knowledge, no publications have systematically discussed the heat sources of HDR, and, instead, most attention has been paid to the technological issues in hydraulic fracturing.

Previous work has focussed on the cataloging of geothermal play types based on geologic controls. For example, Moeck (2014) divided the geothermal play into two types: convection-dominated, and conduction dominated; he further created sub-catalogs based on the existence of a magma heat source. In addition, this and other work reviewed the heat sources that might contribute to a typical geothermal field (Moeck, 2014; Wang, 2015), all of which led us to the idea of making a new catalog on HDR geothermal systems based on heat sources.

In this work, we will classify heat sources into two types (with 5 sub-types) and attribute the known HDR/ EGS projects to the heat sources. Then we will discuss how to identify the heat source to provide a reference for the future exploration of HDR geothermal resources.

2 Catalog based on Heat Sources

The common heat sources on the earth are magma, radiogenic heat production, volcanos, tectonic events, etc., but these sources are sometimes ‘concept-crossed’, which makes it difficult to make a classification. A new catalog should be clear and easy to use, providing new help for the exploration of HDR geothermal resources. Actually, different heat sources always have different behaviors affecting the heat transfer and thus have different temperature logging curves.

We correlated five typical borehole temperature logging curves from global EGS projects with different heat sources, as shown in Fig. 1. The graph shows that the

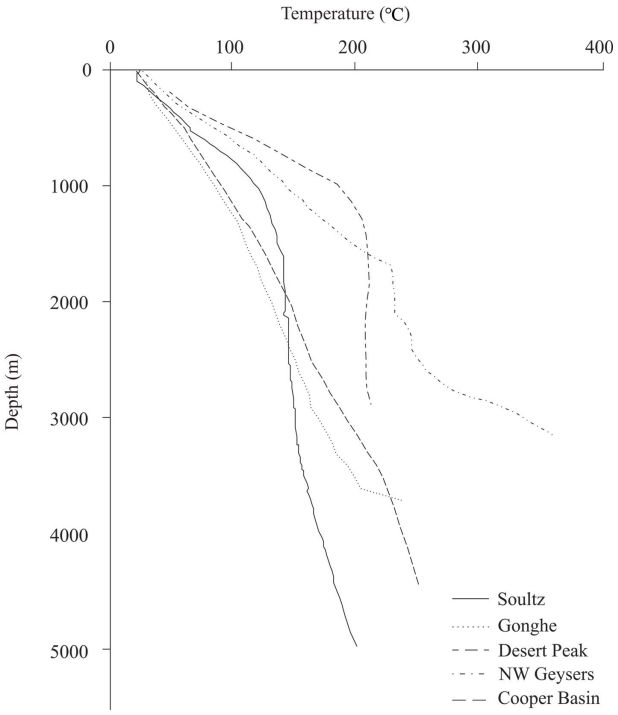

Fig. 1. Temperature logging curves of EGS projects with different heat sources at the typical sites of Soultz (Tenzer et al., 2010), Desert Peak (Robertson-Tait et al., 2005), Gonghe (Zhang, 2019), Northwest Geysers (Garcia et al., 2012), and Cooper Basin (Hogarth and Bour, 2015).

Northwest Geysers EGS project in the USA with a mantle-origin magmatic heat source has a sudden change of temperature (Garcia et al., 2012); the Cooper Basin EGS project in the central Australia, with a heat source from radiogenic heat production illustrates a typical conductive feature of an oblique line (Hogarth and Bour, 2015); the Gonghe EGS project in NE Qinghai-Tibet (e.g. Zhang et al., 2018), has a similar conductive feature but with a sudden change of temperature, with heat sources from partial melting in the crust, radiogenic heat production and heat conducted from the mantle (Zhang, 2019; Kong et al., 2020a); the Desert Peak EGS project in the Nevada, USA, with a major heat source of tectonic events, shows a typical convective feature of a low temperature gradient in the geothermal reservoir (Robertson-Tait et al., 2005); and the Soultz EGS project in France has a major heat source conducted from the mantle and the radiogenic heat production has a lower temperature gradient than other projects (Tenzer et al., 2010). This means that a catalog based on heat sources can help us understand the heat transfer processes and provide guidance for future exploration and resources assessment of HDR.

Therefore, in contrast to a previous catalog based on the geological control (e.g., Moeck, 2014), we make one catalog based only on heat sources. The two major types of heat sources are crust-origin and mantle-origin. We present sub-types below.

2.1 Crust-origin

This type includes three sub-types of partial melting,

non-magma-generated tectonic events, and radiogenic heat production (Fig. 2).

2.1.1 Partial melting

Magma is the molten rock beneath the earth's crust. While most of the magma stays in the mantle, some can also be generated in the crust by the friction induced by tectonic events, including isothermal decompression after plate collision, crustal deformation, and large fault activity (Fig. 2a). The heat can be conducted from the magma/partial melting to an upper reservoir to form HDR geothermal resources that might be exploited. As heat conduction declines with time, the magma's magnitude, temperature, depth, and formation time become the most important parameters to identify whether it will serve as the heat source of geothermal resources.

2.1.2 Non-magma-generated tectonic events

Some tectonic events do not generate enough heat to form magma or even partial melting (Fig. 2b), but still contribute to the formation of geothermal energy. The younger and stronger the tectonic event, the more contribution will be done. However, these kinds of friction always contribute little to the total heat budget.

2.1.3 Radiogenic heat production

Heat can be generated by the decay of radioactive isotopes, including uranium, thorium, potassium, and their daughter nuclides (Fig. 2c). These isotopes are enriched in the upper crust, especially in granitic rocks. This is one of the reasons that most HDR geothermal resources are extracted from granite (see Table 1).

2.2 Mantle-origin

This type is further classified into two sub-types of magma based on heat conducted from the mantle (Fig. 3).

2.2.1 Magma

Magma can be found in various settings, including plate collision zones, subduction zones, continental rift zones, mid-ocean ridges, and hotspots (Fig. 3a). Following the ascent of the magma, it might feed a volcano to be extruded as lava, solidify underground to form an intrusion, or stay as hot spots reaching shallower depth (McBirney and Noyes, 1979). All the magmas mentioned earlier might heat the rock around them. As with the magma heat source in the crust, the magnitude, temperature, depth, and formation time of the magma are very important parameters in determining the heat resource amount. That is why the heat conducted from a Cenozoic volcano is attached importance, whereas the older volcanos are generally considered to contribute little heat now to modern geothermal reservoirs.

2.2.2 Heat conducted from the mantle

In some of the rift systems or basins, there are no magma intrusion events that contribute to the heat accumulation, and even the faults are too old to generate the heat. However, the geothermal resources are still there due to the thin crust or low Moho surface, where the heat can be conducted from the mantle (Fig. 3b).

3 Global EGS Projects Attributed to the Heat Source Catalog

The EGS is an artificial system to explore the geothermal energy from an HDR or low permeability reservoir. While the HDR geothermal resources with no fluid circulation or hydrothermal alteration events are quite few, we instead archive here the EGS worldwide and differentiate them based on the heat sources catalog built in this work.

A total of 35 EGS projects around the world were

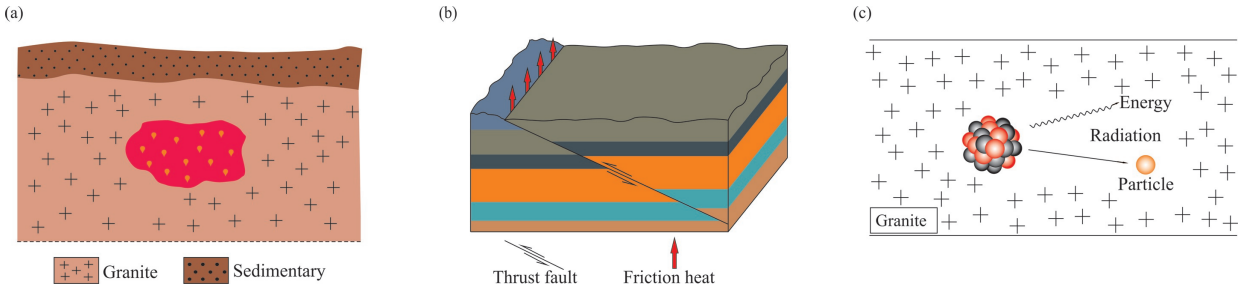

Fig. 2. Crust-origin heat sources: (a) partial melting; (b) non-magma-generated tectonic events; (c) radiogenic heat production.

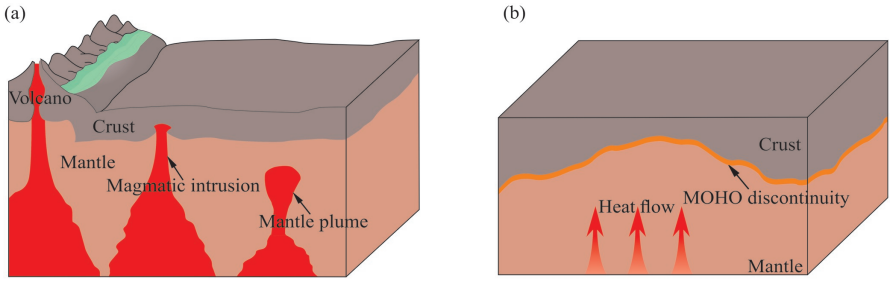

Fig. 3. Mantle-origin heat sources: (a) magma mantle plume and Cenozoic volcano; (b) non-magma heat conducted from the mantle.

considered and classified to create the new catalog, as shown in Fig. 4. We collect the heat flow, reservoir temperature, well depth, rock type and heat source data at each EGS site, and add them to our new catalog system (Table 1). It is already known that all EGS projects have heat sources of radiogenic heat production in the crust and heat conducted from the mantle, but these sources may contribute little to the total heat budget. Thus, we only list the important or major heat sources when assigning them for each project. Because each project could have several major heat sources, we sequence them by order of heat contribution. For example, at the Nesjavellir site in Iceland (Flóvenz and Saemundsson, 1993), the mantle-origin magma is the most important heat source, with the other major source being radiogenic heat production. Thus, in Table 1, we list them in the order of mantle-origin magma and radiogenic heat production.

Using statistics from the 35 projects, there are nine host crust-origin heat source (1 partial melting; 5 non-magma-generated tectonic events; and 3 radiogenic heat production), 25 host mantle-origin heat source (11 magma; 14 non-magma heat conducted from the mantle), and one was not determined due to lack of data. The 25 major reservoirs are granite, and the rest are sandstone and metamorphic rocks.

4 Implications for Hot Dry Rock Exploration

The most important target is to identify potential HDR sites based on analysis of heat sources. Differences in the heat sources might lead to different ways in geological, geophysical and geochemical exploration. In addition, heat source identification is very helpful in geodynamic research. So, where should the HDR target be? And how to identify the heat sources? In this section, we will try to answer these questions.

Table 1 Catalog with statistics of 35 enhanced geothermal systems worldwide

No.	EGS site	Country	Heat flow (mW/m^2)	Reservoir temperature (°C)	Well depth (m)	Rock type	Heat source	Reference
1	Cooper Basin	Australia	100	242–278	4421	Granite	3	Majer et al., 2007; Hogarth and Bour, 2015;
2	Paralana	Australia	100	171	4003	Metasediments, granite	3	Petratherm, 2012
3	Altheim	Austria	\	106	2165–2306	Limestone	2, 3, 5	Pernecker and Ruhland, 1996
4	Yilan	China	108.8	\	\	Shale and sandstone	4, 3	Chan et al., 2018; Fuchs, 2021
5	Gonghe	China	102.2	180	2886	Granite	1, 3, 2	Zhang, 2019
6	Soultz	France	190–167	165	5093	Granite	5, 3	Kappelmeyer, 1967; Gable, 1980; Lucazeau et al., 1991; Tester et al., 2006
7	Bouillante	France	100–101	250–260	1000–2500	Volcanic lavas and tuffs	4, 3	Bertini et al., 2006; Manga et al., 2012; Raguenel et al., 2019;
8	Genesys Hannover	Germany	77	160	3900	Bunter sandstone	5, 3	Zimmermann et al., 2009
9	Groß Schönebeck	Germany	75	145	4309	Sandstone and andesitic volcanic	5, 3	Norden et al., 2008; Zimmermann et al., 2009
10	Mauerstetten	Germany	64	130	4545	Limestone	5, 3	Čermák, 1979; Schrage et al., 2012
11	Bruchsal	Germany	110	123	1874–2542	Bunter sandstone	5, 3	KIT, 2013; Genter et al, 2016
12	Landau	Germany	111–139	159	3170–3300	Granite, carbonates and sandstones	5, 3	Čermák, 1979; Lacirignola and Blanc, 2013
13	Insheim	Germany	\	165	3600–3800	Sandstone, granite	5, 3	Breede et al., 2013
14	Neustadt Glewe	Germany	52	99	2320	Sandstone	5, 3	Stober, 2011; Fuchs, 2021
15	Unterhaching	Germany	75	123	3350–3580	Limestone	5, 3	Čermák, 1979; Wolfgramm, 2007
16	Genesys Horstberg	Germany	73–77	150	3800	Sandstone	5, 3	Schrage et al., 2012; Jung et al., 2019; Fuchs, 2021
17	Bad Urach	Germany	86	143–170	3334–4445	Gneiss	\	Tenzer et al., 2000
18	Rittershoffen	Germany	\	\	\	\	5, 3	
19	Nesjavellir	Iceland	159–170	\	\	\	4, 3	Flóvenz and Saemundsson, 1993
20	Lardarello	Italy	242–574	300–350	2500–4000	Metamorphic rocks	4, 3	Boldizsár, 1963; Minissale, 1991
21	Hijiori	Japan	120; 178; 135; 245	190	1805–1910	Granodiorite	4, 3	Sasaki, 1998
22	Ogachi	Japan	120–140	60–228	400–1100	Granodiorite	4, 3	Kaieda et al., 2010
23	Pohong	South Korea	90–100	140	\	Granodiorite	5, 3	Lee et al., 2011
24	Fjallbacka	Sweden	<65	16	70–500	Granite	5	Portier et al., 2007
25	St. Gallen	Switzerland	\	130–150	4450	Malm, shell limestone	2, 5	Omodeo-Salé et al., 2020; Fuchs, 2021
26	Basel	Switzerland	80–100	190–200	5000	Granite	5, 3	Ladner and Häring, 2009
27	Rosemanowes	UK	120	79–100	2000–2600	Granite	3	Tester et al., 2006
28	Berlín	USA	\	183	2000–2380	Volcanic rocks	4, 3	Monterrosa and Santos, 2013
29	Coso	USA	83–196	≥300	2430–2956	Diorite granodiorite granite	4, 3	Combs, 1980; Rose et al., 2014
30	Desert Peak	USA	422.2	179–196	1067	Volcanic and metamorphic rocks	2, 3, 5	Blackwell and Richards, 2004; Chabora et al., 2012
31	Newberry	USA	221.4	315	3066	Volcanic rocks	4, 3	Fittermann, 1988; Blackwell and Richards, 2004
32	NW Geysers	USA	150	~400	3396	Metasedimentary rocks	4, 3	Romero et al., 1995; Garcia et al., 2012
33	Fenton Hill	USA	130–200	200–327	2932–4390	Crystalline rock	4, 3	Brown, 2009
34	Raft River	USA	150	140	\	Granite	2, 3	Bradford et al., 2013; Fuchs, 2021
35	Bradys Hot Spring	USA	99–247	\	\	Rhyolite, metamorphic substrate	2, 3, 5	Blackwell and Richards, 2004

Heat source 1–5 = crustal partial melting, non-magma-generated tectonic events, radiogenic heat production, mantle-origin magma, and heat conducted from the mantle, respectively

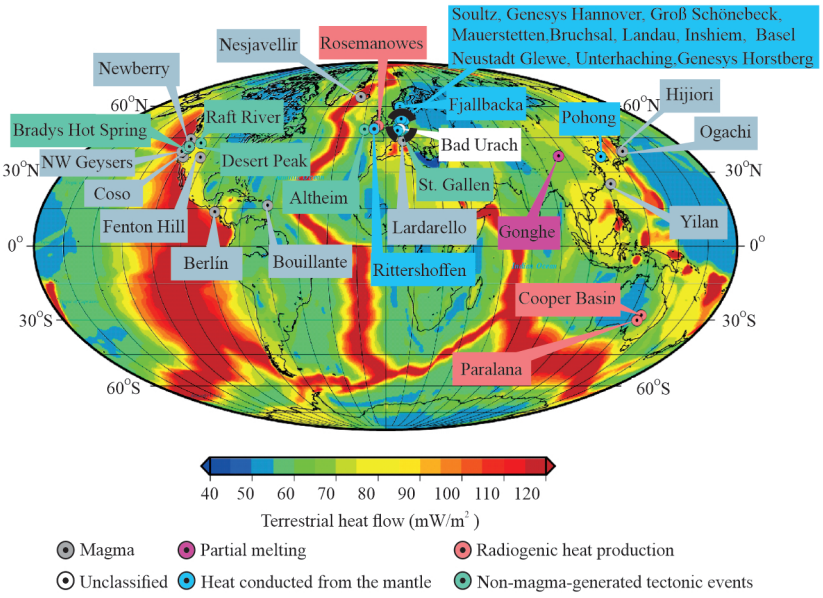

Fig. 4. EGS projects on the global heat flow map (EGS sites are marked by different colors to show their heat source). Heat flow map modified from Lucazeau (2019).

4.1 Finding the HDR target

Based on the new catalog, we can find that most (71%) of the EGS projects have dominant heat sources of mantle-origin plus radiogenic heat production. And, as mentioned, EGS projects with a heat source of magma in the mantle have the highest temperature. Therefore, the primary type for EGS exploration is magma in the mantle domain type. For this type, the exploration target should focus on the magma's magnitude, temperature, depth, and formation time. For example, Northwest Geysers in California, one of the successful EGS sites, has a major heat source of mantle-origin magma. The temperature of the magma chamber is higher than 700°C, and the depth to the top of the magma chamber is 5000 m (Peacock et al., 2019). This high-quality heat source is the key point for implementing successful EGS projects, but it should be noted that there might be exceptions: the regions near the Cenozoic volcanos can have lower temperatures than expected. For example, in the Changbaishan volcano of northeastern China, the geo-temperature at a depth of 4000 m is less than 150°C where the Cenozoic volcano exists (Pang et al., 2020). The secondary target type is the crust-origin heat source system. The exploration target should pay attention to thick crust with high radiogenic heat production rate. Nevertheless, from the experience of previous successful EGS projects, it is hard to conduct hydraulic stimulation at EGS sites with a major heat source of radiogenic heat production because of the thick crust. In comparison, EGS projects with large-scale faults in rift systems (e.g., Soultz, Desert Peak, and Geysers) are usually successful.

The index of heat flow data, temperature gradient, and heat production rate should be highlighted in the exploration of HDR. Considering together Fig. 4 and Table 1, we can find that:

(1) All EGS projects have a heat flow over 52 mW/m^2, and 83% of them are higher than 100 mW/m^2;

(2) EGS projects with a mantle-origin magma heat source are mainly located in the Circum-Pacific and Atlantic mid-ocean ridge geothermal belts. This type has high heat flow from 83 to 574 mW/m^2 and most of them are higher than 100 mW/m^2;

(3) EGS projects with a major heat source of heat conducted from the mantle are distributed on the boundary of a plate; exactly, they are located in the Rhineland graben and Sweden. This type has heat flow from 52 to 190 mW/m^2, and many are less than 100 mW/m^2;

(4) EGS sites with major heat source generated from tectonic events are also on the edge of plates, but have a higher heat flow than 99 mW/m^2;

(5) EGS sites that host major heat sources of radiogenic heat production are all inside a plate, and their heat flows are between 100 and 120 mW/m^2;

(6) Only the Gonghe Basin hosts a crustal partial melting heat source with heat flow of 102.2 mW/m^2, which is derived from the unique tectonic events of the Tibet Plateau.

Therefore, heat flow with values higher than 100 mW/m^2 should especially be focused upon. Further, as most of the EGS reservoirs are granites, such kinds of reservoirs should be given prime attention.

4.2 Identification of the heat source

Heat sources can be identified based on many methods, including geophysical, geochemical and geological technologies. In terms of the heat source catalog in this paper, we briefly introduce the geophysical and geochemical methods, with more attention to noble gas geochemistry and lithospheric thermal structure analysis, which can lead to the identification of the crust or mantle origin. All methods will be introduced with cases from the EGS projects in section 3.

4.2.1 Geophysical methods

Geophysical investigations play an important role in advancing our understanding of the lithospheric transformation, crustal and mantle structure (Le Pape et al., 2012; Gao et al., 2013, 2020a, b; Zhang et al., 2020). Generally, geophysical investigations are often used to identify magma heat source in the exploration of geothermal resources (Huang et al., 2015; Gao et al., 2020a, b; Pan et al., 2021). It should be noted that a better understanding of geological structure helps to interpret geophysical data. Herein, we summarize briefly the geophysical features of magma heat sources.

The low resistivity and low-velocity zones detected by geophysical methods are usually interpreted as magma chamber, partial melt zone, aqueous fluid and crustal shear zones (Wei et al., 2001; Hacker et al., 2014; Huang et al., 2015; Wang et al., 2016; Gao et al., 2020b). For example, Gao et al. (2020b) interpreted the low resistivity zones (<3 Ω·m) in the middle crust of the Gonghe Basin as partial melt zones. Huang et al. (2015) interpreted the low velocity zones (>5% P-wave velocity reduction) beneath Yellowstone National Park as magma reservoirs. Furthermore, the melt fraction can be estimated using a resistivity model and P-wave and S-wave velocity models (Le Pape et al., 2012; Huang et al., 2015; Gao et al., 2020b). It should be noted that limits of resistivities and velocities to constrain magma heat sources are variable in different regions. Therefore, we should integrate geological and geochemical evidence to make comprehensive conclusions.

4.2.2 Geochemical methods

Volcanic rocks and entrained xenoliths can provide important information about the thermal regime of the crust and upper mantle (Wang et al., 2012b, 2016). Wang et al. (2016) calculated zircon saturation temperatures for magmatic rocks in central and northern Tibet and interpreted the Songpan–Ganzi–central Kunlun rhyolites as being generated by dehydration partial melting of the middle to lower crust at depths of 16–50 km during 9.0–1.5 Ma.

Fluids play a key role in the transportation of heat and mass (Menzies et al., 2014; Jiang et al., 2018; Pan et al., 2021) and provide important information on the heat sources and genesis of geothermal systems (Guo, 2012; Jiang et al., 2019b; Kong et al., 2020b; Pan et al., 2021). The input of magmatic fluids can influence the geochemistry of geothermal fluids in high-temperature geothermal systems with magma heat sources (Guo, 2012, 2020; Guo et al., 2019; Pan et al., 2021). Generally, these geothermal fluids often have high Cl, trace elements, such as B, As, Li, Rb, and Cs concentrations as in e.g., Yangbajing, Tengchong Rehai and Yellowstone National Park (Truesdell and Fournier, 1976; Guo, 2012, 2020; Guo et al., 2019), and ^{2}H, ^{18}O isotope values due to the effects of magmatic volatiles (Liu et al., 2019; Pan et al., 2021).

Noble gas isotope geochemistry can provide heat source analysis by revealing deep fluid origin. As a noble gas, helium is an excellent natural tracer for fluid migration and identifying mantle-derived volatiles (Hoke et al., 2000; Klemperer et al., 2013). Moreover, gas isotopic compositions (e.g., $^{3}He/^{4}He$) respond quickly to tectonic and magmatic processes (Sano et al., 2014; Zhang et al., 2021). ^{3}He is mainly produced within the mantle and is associated with mantle heat flux, while ^{4}He, which is a decay product of U and Th, is mainly concentrated in the continental crust (O'Nions and Oxburgh, 1988). The $^{3}He/^{4}He$ ratio of the crust and mantle is 0.02 Ra and 8 Ra, respectively (Ra is the atmospheric $^{3}He/^{4}He$ ratio = 1.382×10^{-6}; Sano and Wakita, 1985). Thus, helium isotopes can provide evidence for determining the heat flux, which is mainly generated from the crust or mantle. We considered the noble gas isotopes data from the Gonghe Basin and Geysers Basin to illustrate the application of He isotopes; these data are shown in Table 2. $^{4}He/^{20}Ne$ ratios are used to estimate the content of air contamination; we plotted all gas samples in a $^{3}He/^{4}He$ vs. $^{4}He/^{20}Ne$ diagram (Fig. 5). As shown in Fig. 5 and Table 2, the He ratios of all samples in the Gonghe Basin range from 0.01 Ra to 0.18 Ra, indicating that the helium in this basin is mainly from a crustal source. The mantle magmatic ^{3}He signatures have largely been obliterated because they account for no more than 5%, implying that the heat is primarily from the crust. However, the He ratios of gas samples in the Geysers Basin range from 6.7 Ra to 9.5 Ra, indicating that the helium there is mainly from a mantle source. Therefore, the heat in the Geysers Basin was mainly generated from the mantle together with other evidence.

4.2.3 Lithospheric thermal structure analysis

Lithospheric thermal structure refers to the ratio of heat flow in the crust (q_c) and mantle (q_m), as well as the temperature distribution of the lithosphere (Blackwell, 1971; Rudnick et al., 1998). Terrestrial heat flow (q) reflects the combination of heat within the crust and mantle, and thus, is a key parameter to estimate the lithospheric thermal structure (Balling, 1995; Davies and Davies, 2010; Zhang et al., 2018; Jiang et al., 2019a; Feng et al., 2019). Based on Fourier's Law, terrestrial heat flow can be calculated by the following equation (Roy et al., 2008):

$$q = k\frac{\partial T}{\partial Z}$$

where k kis the thermal conductivity of rock samples, T is temperature, and Z is depth.

Therefore, terrestrial heat flow can be determined from the continuous borehole temperature logs and rocks thermal conductivity data (Zhang et al., 2018). Taking the Gonghe Basin as an example, we introduce the principle of lithospheric thermal structure analysis for heat source identification. Based on the temperature logging results, the average temperature gradient of the basement granite from the Gonghe Basin (41.5 °C/km) is obtained (Zhang et al., 2018). With thermal conductivity values at the same depth (2.21–3.03 W/(m·K)), terrestrial heat flow can be calculated (Zhang, 2019). The average heat flow of the Gonghe Basin is 102.2 mW/m^2 (Zhang et al., 2018, 2020). Based on the average heat flow, the lithospheric thermal structures of the Gonghe Basin were revealed by the

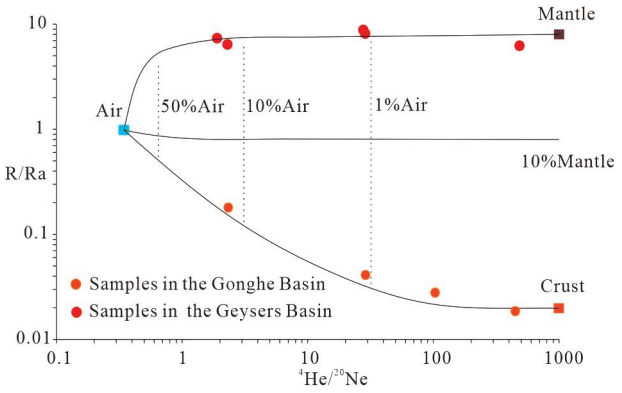

Fig. 5. Principles of noble gas isotope geochemistry in identifying the heat sources, with examples from the Gonghe Basin and Geysers Basin.

Table 2 Measured chemical parameters of noble gases in the Gonghe Basin and Geysers Basin

Sample Sites	$^4He/^{20}Ne$	R/Ra	References
Gonghe	29	0.041	Pan et al., 2021
	2.34	0.180	
	449.91	0.018	
	103.08	0.027	
Geysers	2.3	6.9	Torgerson and Jenkins, 1982
	28	9.5	
	29	8.8	
	498	6.7	

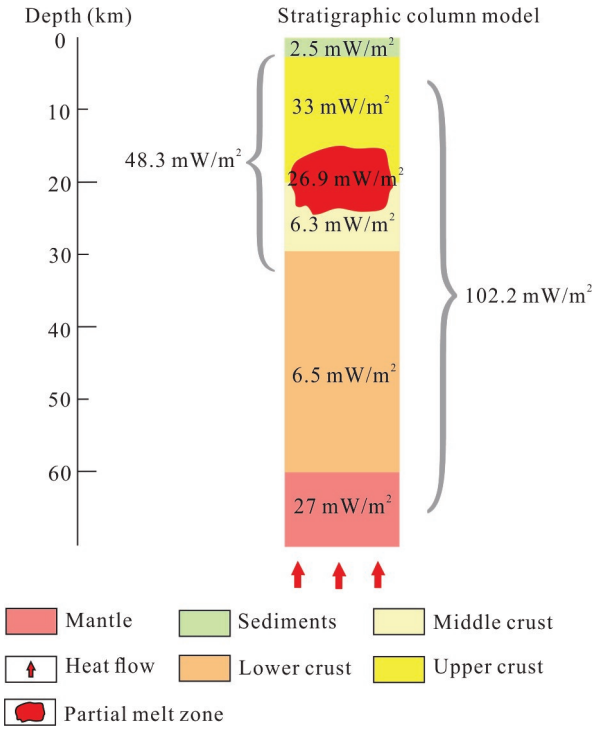

Fig. 6. Lithospheric thermal structure analysis: the contributions of heat production (mW/m^2) from individual heat source to the terrestrial heat flow in the Gonghe Basin (modified after Zhang et al., 2020 and Pan et al., 2021).

crustal heat flow (q_c) and mantle heat flow (q_m). The q_c and q_m values are calculated by the 'stripped-back' method based on the surface heat flow, radiogenic heat production rate and thickness of crustal layering (Majorowicz, 1979). The heat production of the crustal sections is 48.3 mW/m^2, which accounts for 47.3% of the terrestrial heat flow. Furthermore, by applying terrestrial heat flow analysis, Zhang et al. (2020) suggested that the regional mantle heat flow was 27 mW/m^2. The sum of the heat production of the crust and the mantle heat flow is 75.3 mW/m^2, which is not matched by the average heat flow of the Gonghe Basin (102.2 mW/m^2). Thus, there should be an additional heat source, which is approximately 27 mW/m^2 (Zhang et al., 2020) and confirmed by the geochemical and geophysical data as partial melting, as shown in Fig. 6 (Zhang et al., 2020; Pan et al., 2021).

5 Conclusions

We made a new catalog of 35 global Enhanced Geothermal Systems based on two major heat source types of crust-origin and mantle-origin. The former type includes three sub-types of partial melting, non-magma-generated tectonic events, and radiogenic heat production, whereas the latter type includes two sub-types of magma and heat conducted from the mantle. From this classification perspective, we find that 25 EGS projects host mantle-origin heat sources, while only nine EGS projects host crust-origin heat sources among the total EGS projects.

EGS projects with a heat source of magma in the mantle have the highest temperature and high heat flow background, and thus, this heat source type should be regarded as the primary highlight for exploration and development. Then for the crustal heat source region, high radiogenic heat production rate and recent tectonic events turn out to be very important in searching for an exploitation target.

Finally, we have shown how to identify the heat sources based on geophysical and geochemical methods, including noble gas isotope geochemistry and lithospheric thermal structure analysis.

The new catalog is clear and easy to be used and will be helpful in the future exploration and resources assessment of HDR geothermal resources.

Acknowledgements

This work was supported by the National Key Research and Development Program of China (Grant No. 2018YFB1501801) and the Youth Innovation Promotion Association of Chinese Academy of Sciences (No. 2020067). We thank the anonymous reviewers and editors for their nice comments in improving the paper quality. Dr. Susan Turner (Brisbane) is appreciated in polishing the English language.

Manuscript received Jul. 29, 2021
accepted Oct. 25, 2020
associate EIC: XU Tianfu
edited by Susan TURNER and FANG Xiang

References

Balling, N., 1995. Heat flow and thermal structure of the lithosphere across the Baltic Shield and northern Tornquist Zone. Tectonophysics, 244(1–3): 13–50.

Bertini, G., Casini, M., Gianelli, G., and Pandeli, E., 2006. Geological structure of a long-living geothermal system, Larderello, Italy. Terra Nova, 18(3): 163–169.

Blackwell, D.D., 1971. Heat flow. Eos, Transactions American Geophysical Union, 52(5): IUGG-135.

Blackwell, D.D., and Richards, M., 2004. Geothermal Map of North America. Geological Society of America, 6. DOI: 10.1130/DNAG-CSMS-v6.

Stober, I., 2011. Tiefe Geothermie—Nutzungsmöglichkeiten in Deutschland. Federal Ministry for the Environment, Nature Conservation, Building and Nuclear Safety (BMU). https://www.bmu.de/en/.

Boldizsár, T., 1963. Terrestrial heat flow in the natural steam field at Larderello. Geofisica Pura e Applicata, 56(1): 115–122.

Bradford, J., McLennan, J., Moore, J., Glasby, D., Waters, D., Kruwell, R., Bailey, A., Rickard, W., Bloomfield, K., and King, D., 2013. Recent developments at the Raft River geothermal field. In: Proceedings, Thirty-Eighth Workshop on Geothermal Reservoir Engineering, Stanford University, California, USA. https://openei.org/w/images/3/39/Raft1.pdf.

Breede, K., Dzebisashvili, K., Liu, X.L., and Falcone, G., 2013. A systematic review of enhanced (or engineered) geothermal systems: Past, present and future. Geothermal Energy, 1(1): 1–27.

Brown, D.W., 2009. Hot dry rock geothermal energy: Important lessons from Fenton Hill. In: Proceedings, Thirty-fourth Workshop on Geothermal Reservoir Engineering, Stanford University, California, USA. https://pangea.stanford.edu/ERE/pdf/IGAstandard/SGW/2009/brown.pdf.

Čermák, V., 1979. Heat flow map of Europe. Terrestrial heat flow in Europe, 3–40. DOI:10.1007/978-3-642-95357-6_1.

Chabora, E., Zemach, E., Spielman, P., Drakos, P., Hickman, S., Lutz, S., Boyle, K., Falconer, A., Robertson-Tait, A., Davatzes, N.C., Rose, P., Majer, E., and Jarpe, S., 2012. Hydraulic stimulation of well 27–15, Desert Peak geothermal field, Nevada, USA. In: Proceedings, Thirty-seventh Workshop on Geothermal Reservoir Engineering, Stanford University, California, USA. https://www.researchgate.net/publication/262301591_Hydraulic_Stimulation_of_Well_27-15_Desert_Peak_Geothermal_Field_Nevada_USA.

Chan, H.P., Chang, C.P., and Dao, P.D., 2018. Geothermal anomaly mapping using Landsat ETM+data in Ilan Plain, northeastern Taiwan. Pure and Applied Geophysics, 175(1): 303–323.

Combs, J., 1980. Heat flow in the Coso geothermal area, Inyo County, California. Journal of Geophysical Research: Solid Earth, 85(B5): 2411–2424.

Davies, J.H., and Davies, D.R., 2010. Earth's surface heat flux. Solid Earth, 1(1): 5–24.

Feng, R.P., Zuo, Y.H., Yang, M.H., Zhang, J., Liu, Z., Zhou, Y.S., and Hao, Q.Q., 2019. Present terrestrial heat flow measurements of the geothermal fields in the Chagan Sag of the YingenEjinaqi Basin, Inner Mongolia, China. Acta Geologica Sinica (English Edition), 93(2): 283–296.

Fittermann, D.V., 1988. Overview of the structure and geothermal potential of Newberry Volcano, Oregon. Journal of Geophysical Research: Solid Earth, 93: 10059–10066.

Flóvenz, Ó.G., and Saemundsson, K., 1993. Heat flow and geothermal processes in Iceland. Tectonophysics, 225(1–2): 123–138.

Fuchs, S., 2021. Global Heat Flow Database: Release 2021. http://www.ihfc-iugg.org/.

Gable, R., 1980. Terrestrial heat flow in France. In: Advances in European Geothermal Research. Springer, Dordrecht, 466–473.

Gao, J., Zhang, H.J., Zhang, H.P., Zhang, S.Q., and Cheng, Z.P., 2020a. Three-dimensional magnetotelluric imaging of the SE Gonghe Basin: Implication for the orogenic uplift in the northeastern margin of the Tibetan plateau. Tectonophysics, 789: 228525.

Gao, J., Zhang, H.J., Zhang, S.Q., Xin, H.L., Li, Z.W., Tian, W., Bao, F., Cheng, Z.P., Jia, X.F., and Fu, L., 2020b. Magma recharging beneath the Weishan volcano of the intraplate wudalianchi volcanic field, northeast china, implied from 3-d magnetotelluric imaging. Geology, 48(9): 913–918.

Gao, R., Wang, H.Y., Yin, A., Dong, S.W., Kuang, Z.Y., Zuza, A.V., Li, W.H., and Xiong, X.S., 2013. Tectonic development of the northeastern Tibetan Plateau as constrained by high-resolution deep seismic-reflection data. Lithosphere, 5(6): 555–574.

Garcia, J., Walters, M., Beall, J., Hartline, C., Pingol, A., Pistone, S., and Wright, M., 2012. Overview of the Northwest Geysers EGS demonstration project. In: Proceedings, Thirty-seventh Workshop on Geothermal Reservoir Engineering, Stanford University, California, USA. https://pangea.stanford.edu/ERE/pdf/IGAstandard/SGW/2012/Garcia.pdf.

Genter, A., Baujard, C., Cuenot, N., Dezayes, C., Kohl, T., Masson, F., Sanjuan, B., Scheiber, J., Eva, S., Schmittbuhl., and Vidal, J., 2016. Geology, Geophysics and Geochemistry in the Upper Rhine Graben: the frame for geothermal energy use. In: Proceedings, European Geothermal Congress, 2016: 5.

Guo, Q.H., 2012. Hydrogeochemistry of high-temperature geothermal systems in China: A review. Applied Geochemistry, 27(10): 1887–1898.

Guo, Q.H., Planer-Friedrich, B., Liu, M.L., Yan, K.T., and Wu, G., 2019. Magmatic fluid input explaining the geochemical anomaly of very high arsenic in some southern Tibetan geothermal waters. Chemical Geology, 513: 32–43.

Guo, Q.H., 2020. Magma-heated geothermal systems and hydrogeochemical evidence of their occurrence. Acta Geologica Sinica, 94(12): 3544–3554 (in Chinese with English abstract).

Hacker, B. R., Ritzwoller, M. H., and Xie, J., 2014. Central Tibet has a partially melted, mica-bearing crust. Tectonics, 33: 1408–1424.

Hogarth, R.A., and Bour, D., 2015. Flow performance of the Habanero EGS closed loop. In: Proceedings, World Geothermal Congress, Melbourne, Australia. https://www.researchgate.net/publication/292137874_Flow_Performance_of_the_Habanero_EGS_Closed_Loop.

Hoke, L., Lamb, S., Hilton, D.R., and Poreda, R.J., 2000. Southern limit of mantle-derived geothermal helium emissions in Tibet: Implications for lithospheric structure. Earth and Planetary Science Letters, 180(3–4): 297–308.

Huang, H.H., Lin, F.C., Schmidt, B., Farrell, J., Smith, R.B., and Tsai, V.C., 2015. The Yellowstone magmatic system from the mantle plume to the upper crust. Science, 348(6236): 773–776.

Huang, S.P., and Liu, J.Q., 2010. Geothermal energy stuck between a rock and a hot place. Nature, 463(7279): 293.

Huttrer, G.W., 2020. Geothermal power generation in the world 2015-2020 update report. In: Proceedings, World Geothermal Congress, Reykjavik, Iceland, 17. https://geothermie-schweiz.ch/wp_live/wp-content/uploads/2020/09/Huttrer_2020_Geothermal_Power_Generation_worldwide-2020_update-report.pdf.

Jiang, G.Z., Hu, S.B., Shi, Y.Z., Zhang, C., Wang, Z.T., and Hu, D., 2019a. Terrestrial heat flow of continental China: Updated dataset and tectonic implications. Tectonophysics, 753: 36–48.

Jiang, Z., Xu, T., Mallants, D., Tian, H., and Owen, D.D., 2019b. Numerical modelling of stable isotope (^{2}H and ^{18}O) transport in a hydro-geothermal system: Model development and implementation to the Guide Basin, China. Journal of Hydrology, 569: 93–105.

Jiang, Z., Xu, T., Owen, D. D. R., Jia, X., Feng, B., and Zhang, Y., 2018. Geothermal fluid circulation in the Guide Basin of the northeastern Tibetan Plateau: isotopic analysis and numerical modeling. Geothermics, 71: 234–244.

Jolie, E., Scott, S., Faulds, J., Chambefort, I., Axelsson, G., Gutiérrez-Negrín, L.C., Regenspurg, S., Ziegler, M., Ayling, B., Richter, A., and Zemedkun, M.T., 2021. Geological controls on geothermal resources for power generation. Nature

Review Earth and Environment, 2(5): 324–339.
Jung, R., Hassanzadegan, A., and Tischner, T., 2019. Determination of hydraulic properties of a large self-propped hydraulic fracture in the geothermal research borehole Horstberg Z1 in the Northwest German Basin. Geothermal, 2019: 1–33.
Kaieda, H., Sasaki, S., and Wyborn, D., 2010. Comparison of characteristics of micro-earthquakes observed during hydraulic stimulation operations in Ogachi, Hijiori and Cooper Basin HDR projects. In: Proceedings, World Geothermal Congress, Bali, Indonesia. https://www.geothermal-energy.org/pdf/IGAstandard/WGC/2010/3157.pdf.
Kappelmeyer, O., 1967. The geothermal field of the Upper Rhinegraben. Pascal and Francis Bibliographic Databases. https://pascal-francis.inist.fr/vibad/.
Karlsruher Institute für Technologie (KIT), 2013. Langzeitbetrieb und Optimierung eines Geothermiekraftwerks in einem geklüftet-porösen Reservoir im Oberrheingraben (LOGRO). http://www.agw.kit.edu/908_998.php.
Klemperer, S.L., Kennedy, B.M., Sastry, S.R., Makovsky, Y., Harinarayana, T., and Leech, M.L., 2013. Mantle fluids in the Karakoram fault: Helium isotope evidence. Earth and Planetary Science Letters, 366(1): 59–70.
Kong, Y.L., Pan, S., and Zhang, C., 2020a. Heat sources of hot dry rock in the Gonghe Basin, Northeastern Tibetan Plateau, In: Proceedings, World Geothermal Congress, Reykjavik, Iceland. https://pangea.stanford.edu/ERE/db/WGC/Abstract.php?PaperID=6015.
Kong, Y.L., Pang, Z.H., Pang, J.M, Li, J., Lyu, M., and Pan, S., 2020b. Fault-affected fluid circulation revealed by hydrochemistry and isotopes in a large-scale utilized geothermal reservoir. Geofluids, 2020(24): 1–13.
Kumari, W.G.P., and Ranjith, P.G., 2019. Sustainable development of enhanced geothermal systems based on geotechnical research — A review. Earth-Science Reviews, 199: 102955.
Lacirignola, M., and Blanc, I., 2013. Environmental analysis of practical design options for enhanced geothermal systems (EGS) through life-cycle assessment. Renewable energy, 50: 901–914.
Ladner, F., and Häring, M.O., 2009. Hydraulic characteristics of the Basel 1 enhanced geothermal system. GRC Transactions, 33: 199–203.
Lee, T.J., Song, Y., Yoon, W.S., Kim, K.Y., Jeon, J., Min, K.B., and Cho, Y.H., 2011. The first enhanced geothermal system project in Korea. In: Proceedings, Ninth Asian Geothermal Symposium, Japan, 4. http://citeseerx.ist.psu.edu/viewdoc/download?doi=10.1.1.1058.268&rep=rep1&type= pdf.
Le Pape, F., Jones, A.G., Vozar, J., and Wei, W.B., 2012. Penetration of crustal melt beyond the Kunlun fault into northern Tibet. Nature Geoscience, 5(5): 330–335.
Liu, M.L., Guo, Q.H, Wu, G., Guo, W., She, W.Y., and Yan, W.D., 2019. Boron geochemistry of the geothermal waters from two typical hydrothermal systems in Southern Tibet (China): Daggyai and Quzhuomu. Geothermics, 82: 190–202.
Lucazeau, F., 2019. Analysis and mapping of an updated terrestrial heat flow data set. Geochemistry, Geophysics, Geosystems, 20(8): 4001–4024.
Lucazeau et al., 1991. Trends of Heat Flow Density from West Africa. In: Terrestrial Hest Floe and the Lithosphere Structure, Springer, Berlin, Heidelberg, 417–425. DOI: 10.1007/978-3-642-75582-8_20.
Lund, J.W., and Toth, A.N., 2020. Direct utilization of geothermal energy 2020 worldwide review. Geothermics, 90: 101915.
Majer, E.L., Baria, R., Stark, M., Oates, S., Bommer, J., Smith, B., and Asanuma, H., 2007. Induced seismicity associated with enhanced geothermal systems. Geothermics, 36(3): 185–222.
Majorowicz, J., 1979. Mantle heat flow and geotherms for major tectonic units in Central Europe. Geothermics and Geothermal Energy, Birkhäuser, Basel, 109–123.
Manga, M., Hornbach, M.J., Le Friant, A., Ishizuka, O., Stroncik, N., Adachi, T., Aljahdali, M., Boudon, G., Breitkreuz, C., Fraass, A., Fujinawa, A., Hatfield, R., Jutzeler, M., Kataoka, K., Lafuerza, S., Maeno, F., Martinez-Colon, M., Mccanta, M., Morgan, S., Palmer, M.P., Saito, T., Slagle, A., Stinton, A.J., Subramanyam, K.S.V., Tamura, Y., Talling, P.J., Villemant, B., Wall-Palmer, D., and Wang, F., 2012. Heat flow in the Lesser Antilles Island arc and adjacent back arc Grenada basin. Geochemistry, Geophysics, Geosystems, 13(8): Q08007.
McBirney, A.R., and Noyes, R.M., 1979. Crystallization and layering of the Skaergaard intrusion. Journal of Petrology, 20 (3): 487–554.
Menzies, C.D., Teagle, D.A., Craw, D., Cox, S.C., Boyce, A.J., Barrie, C.D., and Roberts, S., 2014. Incursion of meteoric waters into the ductile regime in an active orogen. Earth and Planetary Science Letters, 399: 1–13.
Minissale, A., 1991. The Larderello geothermal field: A review. Earth-Science Reviews, 31(2): 133–151.
Moeck, I. S., 2014. Catalog of geothermal play types based on geologic controls. Renewable and Sustainable Energy Reviews, 37: 867–882.
Monterrosa, M., and Santos, P., 2013. Conceptual models for the Berlin geothermal field, case history. In: Proceedings, Short Course V on Conceptual Modeling of Geothermal Systems, Santa Tecla organized by UNU-GTP and LaGeo, Santa Tecla, El Salvador. https://orkustofnun.is/gogn/unu-gtp-sc/UNU-GTP-SC-16-28.pdf.
Norden, B., Förster, A., and Balling, N., 2008. Heat flow and lithospheric thermal regime in the Northeast German Basin. Tectonophysics, 460(1–4): 215–229.
Omodeo-Salé, S., Eruteya, O.E., Cassola, T., Baniasad, A., and Moscariello, A., 2020. A basin thermal modelling approach to mitigate geothermal energy exploration risks: The St. Gallen case study (eastern Switzerland). Geothermics, 87: 101876.
O'Nions, R.K., and Oxburgh, E.R., 1988. Helium, volatile fluxes and the development of continental crust. Earth and Planetary Science Letters, 90(3): 331–347.
Pan, S., Kong, Y.L., Wang, K., Ren, Y.Q., Pan, Z.H., Zhang, C., Wen, D.G., Zhang, L.Y., Feng, Q.D., Zhu, G.L., and Wang, J.Y., 2021. Magmatic origin of geothermal fluids constrained by geochemical evidence: Implications for the heat source in the northeastern Tibetan Plateau. Journal of Hydrology, 603: 126985.
Pang, Z.H., Luo, J., Cheng, Y.Z., Duan, Z.F., Tian, J., Kong, Y.L., Li, Y.M., Hu, S.B., and Wang, J.Y., 2020. Evaluation of geological conditions for the development of deep geothermal energy in China (in Chinese). Earth Science Frontiers, 27(1): 134–151.
Peacock, J.R., Mangan, M.T., Walters, M., Hartline, C., Glen, J.M., Earney, T.E., and Schermerhorn, W.D., 2019. Geophysical characterization of the heat source in the Northwest Geysers, California. In: Proceedings, 44th Workshop on Geothermal Reservoir Engineering, Stanford University, California, USA. https://pubs.er.usgs.gov/publication/70202299.
Pernecker, G., and Ruhland, J., 1996. Altheim geothermal plant for electricity production by organic rankine cycle turbogenerator. In: Proceedings, Twenty-first Workshop on Geothermal Reservoir Engineering, Stanford University, California, USA. https://www.osti.gov/biblio/889717.
Petratherm, 2012. Paralana. http://www.petratherm.com.au/projects/paralana.
Portier, S., André, L., and Vuataz, F.D., 2007. Review on chemical stimulation techniques in oil industry and applications to geothermal systems. Engine, work package, 4: 32.
Raguenel, M., Driesner, T., and Bonneau, F., 2019. Numerical modeling of the geothermal hydrology of the Volcanic Island of Basse-Terre, Guadeloupe. Geothermal Energy, 7(1): 1–16.
Robertson-Tait, A., Morris, C., and Schochet, D., 2005. The Desert Peak East EGS project: A progress report. In: Proceedings, World Geothermal Congress, Antalya, Turkey. https://www.geothermal-energy.org/pdf/IGAstandard/WGC/2005/1641.pdf.
Romero Jr, A.E., McEvilly, T.V., Majer, E.L., and Vasco, D., 1995. Characterization of the geothermal system beneath the

Northwest Geysers steam field, California, from seismicity and velocity patterns. Geothermics, 24(4): 471–487.
Rose, P., Sheridan, J., McCulloch, J., Moore, J.N., Kovac, K., Weidler, R., and Hickman, S., 2005. The Coso EGS project-Recent developments. In: Geothermal Resources Council 2005 Annual Meeting, 125–129.
Roy, S., Ray, L., Bhattacharya, A., and Srinivasan, R., 2008. Heat flow and crustal thermal structure in the Late Archaean Closepet Granite batholith, south India. International Journal of Earth Sciences, 97(2): 245–256.
Rudnick, R.L., McDonough, W.F., and O'Connell, R.J., 1998. Thermal structure, thickness and composition of continental lithosphere. Chemical Geology, 145(3–4): 395–411.
Sano, Y., and Wakita, H., 1985. Geographical distribution of $^{3}He/^{4}He$ ratios in Japan: Implications for arc tectonics and incipient magmatism. Journal of Geophysical Research: Solid Earth, 90(B10): 8729–8741.
Sano, Y., Hara, T., Takahata, N., Kawagucci, S., Honda, M., Nishio, Y., Tanikawa, W., Hasegawa, A., and Hattori, K., 2014. Helium anomalies suggest a fluid pathway from mantle to trench during the 2011 Tohoku-Oki earthquake. Nature Communication, 5(1): 1–6.
Sasaki, S., 1998. Characteristics of microseismic events induced during hydraulic fracturing experiments at the Hijiori hot dry rock geothermal energy site, Yamagata, Japan. Tectonophysics, 289(1–3): 171–188.
Schrage, C., Bems, C., Kreuter, H., Hild, S., and Volland, S., 2012. Overview of the enhanced geothermal energy project in Mauerstetten, Germany. https://www.ta-survey.nl/index.php?id=109&lang=EN.
Tenzer, H., Park, C.H., Kolditz, O., and McDermott, C.I., 2010. Application of the geomechanical facies approach and comparison of exploration and evaluation methods used at Soultz-sous-Forêts (France) and Spa Urach (Germany) geothermal sites. Environmental Earth Sciences, 61(4): 853–880.
Tenzer, H., Schanz, U., and Homeier, G., 2000. HDR research programme and results of drill hole Urach 3 to depth of 4440 m–the key for realisation of a hdr programme in southern Germany and northern Switzerland. In: Proceedings World Geothermal Congress, 3927–3932. https://pangea.stanford.edu/ERE/pdf/IGAstandard/EGC/1999/Tenzer2.pdf.
Tester, J.W., Anderson, B.J., Batchelor, A.S., Blackwell, D.D., DiPippo, R., and EM, D., 2006. The Future of Geothermal Energy Impact of Enhanced Geothermal Systems on the United States in the 21st Century. Report prepared by the Massachusetts Institute of Technology for the US Department of Energy. Washington, DC, 4–37.
Tomac, I., and Sauter, M., 2018. A review on challenges in the assessment of geomechanical rock performance for deep geothermal reservoir development. Renewable and Sustainable Energy Reviews, 82: 3972–3980.
Torgersen, T., and Jenkins, W.J., 1982. Helium isotopes in geothermal systems: Iceland, The Geysers, Raft River and Steamboat Springs. Geochimica et Cosmochimica Acta, 46 (5): 739–748.
Truesdell, A.H., and Fournier, R.O., 1976. Conditions in the deeper parts of the hot spring systems of Yellowstone National Park, Wyoming. U.S. Geological Survey Open File Report, 76–428. https://www.osti.gov/biblio/7321574.
Wang, J.Y., 2015. Geothermics and its Applications. Beijing: Science Press (in Chinese).
Wang, J.Y., Hu, S.B., Pang, Z.H., He, L.J., Zhao, P., Zhu, C.Q., Rao, S., Tang, X.Y., Kong, Y.L., Luo, L., and Li, W.W., 2012a. Estimate of geothermal resources potential for hot dry rock in the continental area of China. Science and Technology Review, 30(32): 25–31.
Wang, Q., Chung, S.L., Li, X.H., Wyman, D., Li, Z.X., Sun, W.D., Qiu, H.N., Liu, Y.S., and Zhu, Y.T., 2012b. Crustal melting and flow beneath northern Tibet: Evidence from Mid-Miocene to Quaternary strongly peraluminous rhyolites in the southern Kunlun range. Journal of Petrology, 53(12): 2523–2566.
Wang, Q., Hawkesworth, C.J., Wyman, D., Chung, S.L., Wu, F.Y., Li, X.H., Li, Z.X., Gou, G.N., Zhang, X.Z., Tang, G.J., Dan, W., Ma, L., and Dong, Y.H., 2016. Pliocene-Quaternary crustal melting in central and northern Tibet and insights into crustal flow. Nature Communication, 7(1): 1–11.
Wei, W.B., Unsworth. M., Jones, A., Booker, J., Tan, H.D., Nelson, D., Chen, L.S., Li, S.H., Solon, K., Bedrosian, P., Jin, S., Deng, M., Ledo, J., Kay, D., and Roberts, B., 2001. Detection of widespread fluids in the Tibetan crust by magnetotelluric studies. Science, 292: 716–718.
Wolfgramm, M., Bartels, J., Hoffmann, F., Kittl, G., Lenz, G., Seibt, P., Schulz, R., Thomas, R., and Unger, H.J., 2007. In: Proceedings, European Geothermal Congress, 2007: 1–6.
Zhang, C., 2019. Geothermal characteristics and genesis mechanism of Hot Dry Rock geothermal resources of Gonghe basin, northeastern Tibetan Plateau (Ph.D. thesis). Beijing: University of Chinese Academy of Sciences, 1–124.
Zhang, C., Jiang, G.Z., Shi, Y.Z., Wang, Z.T., Wang, Y., Li, S.T., Jia, X.F., and Hu, S.B., 2018. Terrestrial heat flow and crustal thermal structure of the Gonghe-Guide area, northeastern Qinghai-Tibetan plateau. Geothermics, 72: 182–192.
Zhang, C., Hu, S.B., Zhang, S.S., Li, S.T., Zhang, L.Y., Kong, Y.L., Zuo, Y.H., Song, R.C., Jiang, G.Z., and Wang, Z.T., 2020. Radiogenic heat production variations in the Gonghe Basin, northeastern Tibetan Plateau: Implications for the origin of high-temperature geothermal resources. Renewable Energy, 148: 284–297.
Zhang, H.W., Li, T.D., He, R.Z., Yang, H., Niu, X., and Zuo, C.Q., 2020. Tomographic imaging of the India-Asia Plate collisional tectonics and mantle upwelling beneath western Tibet. Acta Geologica Sinica (English Edition), 94(4): 1159–1166.
Zhang, M.L., Guo, Z.F., Xu, S., Barry, P.H., Sano, Y., Zhang, L.H., Halldórsson, S.A., Chen, A.T., Chen, Z.H., Liu, C.Q., Li, S.L., Lang, Y.C., Zheng, G.D., Li, Z.P., Li, L.W., and Li, Y., 2021. Linking deeply-sourced volatile emissions to plateau growth dynamics in southeastern Tibetan Plateau. Nature Communication, 12(1): 1–10.
Zimmermann, G., Tischner, T., Legarth, B., and Huenges, E., 2009. Pressure-dependent production efficiency of an enhanced geothermal system (EGS): Stimulation results and implications for hydraulic fracture treatments. Rock Physics and Natural Hazards, 1089–1106.

About the first and corresponding author

KONG Yanlong, male; Ph.D., graduated from University of Chinese Academy of Sciences; associate professor; his research interests focus on geothermal reservoir engineering, isotope hydrology and hydrogeology.